J Mol Model (2001) 7:257–264
DOI 10.1007/s008940100039

ORIGINAL PAPER

Nurcan Şenyurt Tüzün · Viktorya Aviyente
Duygu Avcı · Nilsun İnce

A computational approach to the polymerizabilities of diallylamines

Received: 10 January 2001 / Accepted: 21 May 2001 / Published online: 21 July 2001

Abstract Some selected diallylamine monomers have been studied with the semiempirical PM3 method as model compounds for *N*,*N*-dialkyl-*N*-2-(alkoxycarbonyl) allylammonium salts, in order to build up a quantitative and qualitative relationship between the experimental cyclopolymerizabilities of the monomers and calculated parameters such as charge, energy, geometrical features, bond orders, local softness values and HOMO–LUMO gaps. The charges on nitrogen, vinyl and allyl carbons, the activation barriers, the local softness values and the HOMO–LUMO gaps are found to represent the polymerizability trend of the monomers in general. Three-dimensional structures have been proposed for the reactants and their transition states by geometry optimizations with PM3.

Keywords Cyclopolymerization · Diallylamine · PM3 · Local softness · Free radical polymerization

Introduction

The growing interest in diallylamines in recent years is a consequence of the discovery of the cyclopolymerization of diallyl dimethylammonium chloride (DADMAC) to a water-soluble cyclopolymer. [1] Polydiallyldimethylammonium chloride (PDADMAC) and its derivatives (with their copolymers) have been thoroughly investigated in the past. [2] Reported research on diallylammonium salts covers their kinetic, structural and synthetic aspects, as well as the applicability in industrial operations. [2] Diallylammonium polymers have been widely used in industrial operations, and more than 120 patents related to the applications of PDADMAC or its copolymers are available on the commercial market. [2] The most common applications are in the mining industry, [3, 4, 5] paper manufacturing, [6, 7] water treatment [8, 9, 10, 11, 12] and electrolysis. [13, 14]

Research studies on the reactivity of allyl monomers (CH_2=$CHCH_2X$) have shown that the radical polymerizability depends on the functional group X of the monomer, such that the more powerful an electron donor the X group is, the less reactive is the monomer. [15] Vaidya and Mathias [16] have reported a structure–reactivity relationship for the homopolymerizability of various monoallyl and diallylammine monomers. Mathias et al. have synthesized various diallylamines (Scheme 1) and built up a correlation between ^{13}C NMR chemical shift differences of the vinyl carbons and their polymerizability. The same study includes a relationship between the quantum mechanical (MINDO/3) structural and energetic features of these compounds and their polymerizabilities. It was shown that, as the electron-withdrawing ability of the allylic substituent increases, the β-carbon and γ-carbon peaks shift upfield and downfield, respectively (Scheme 1). This implies that β and γ peaks get closer as

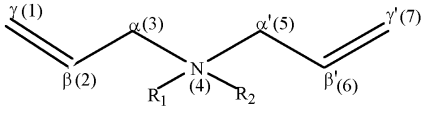

Monomer	R_1	R_2
DAA	H	-
$DAAH^+$	H	H
DADMAC	CH_3	CH_3
DAAP	C_5NH_4	-
$DAAPH^+$	$C_5NH_5^+$	-

Scheme 1 The experimentally investigated monomers [16]

N.Ş. Tüzün · V. Aviyente (✉) · D. Avcı
Boğaziçi University, Faculty of Arts and Science,
Department of Chemistry, 80815, Bebek, İstanbul, Turkey
e-mail: aviye@boun.edu.tr
Tel.: +90-212-2631540, Fax: +90-212-2872467

N. İnce
Boğaziçi University, Institute of Environmental Sciences,
80815, Bebek, İstanbul, Turkey

Table 1 The polymerizability and chemical shift difference $\Delta\delta$ ($=\delta_\gamma-\delta_\beta$) data of diallylamines [16]

R_1	R_2	$\delta_\gamma-\delta_\beta$ (ppm)	Polymerizability
(DADMAC) CH_3	CH_3	3.0	Very good
($DAAH^+$) H	H	3.1	Good
($DAAPH^+$) $C_5NH_5^+$	–	12.4	Moderate
(DAAP) C_5NH_4	–	16.4	Very poor
(DAA) H	–	19.1	Very poor

the electron-withdrawing ability of the allylic substituent increases. Table 1 shows a decrease in chemical shift difference, $\Delta\delta$, between allylic carbons with increasing electron-withdrawing ability of allylic substituents. A smaller chemical shift difference reflects polarization away from the double bond and the connecting CH_2 groups. This reduces chain transfer of hydrogens on the connecting CH_2 groups and high molecular weight polymers are produced. The $\Delta\delta$ values were correlated to the polymerizabilities of the monomers such that monomers with $\Delta\delta$ less than 7.5 ppm were easily polymerized, while those with $\Delta\delta$ values higher than 17 ppm polymerized poorly. The $\Delta\delta$ range from 7.5 to 17 ppm is the transition region from good polymerizability to poor polymerizability. Similar results were observed for ester versus ether derivatives of α-hydroxymethyl acrylates, with the former displaying smaller chemical shift differences and giving much higher molecular weight polymers than the latter. [17]

In the polymerization reaction of diallylamines, the initiator attacks C_1 forming a radical at C_2 (Scheme 2) that may undergo intermolecular reaction with another monomer. The unreacted double bonds can react further to form water-insoluble cross-linked products. Otherwise, the radical at C_2 may attack C_6 or C_7 intramolecularly to form cyclic structures in the polymer backbone. After this cyclization step, the intermolecular propagation step proceeds and the radical formed on the ring attacks

Scheme 2 Radical polymerization reaction for diallylamines

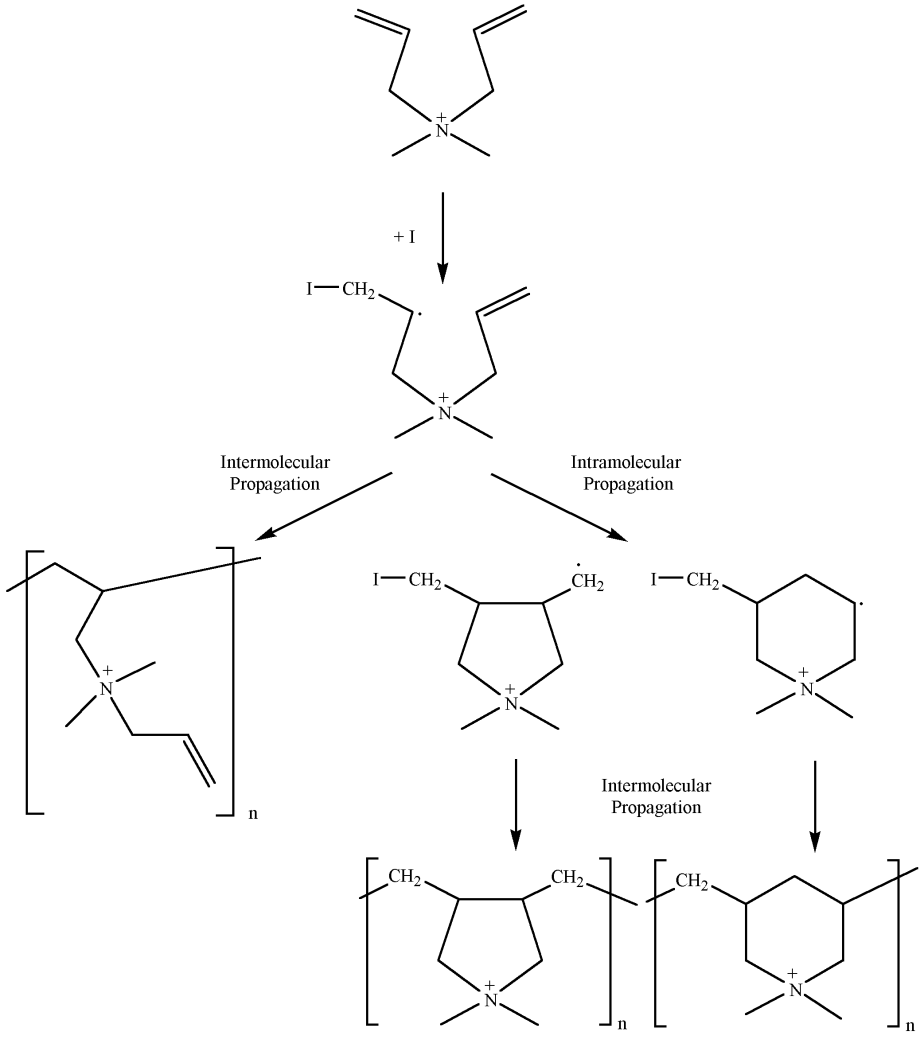

I=Initiator

Fig. 1 A model for the "living monomer"

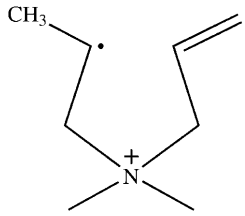

another monomer. This alternating intraintermolecular chain propagation is called "cyclopolymerization".

In the cyclization step of the polymerization reaction, five- or six-membered rings can form depending on the site of attack, C_6 or C_7. The formation of six-membered rings was expected since a six-membered ring is more stable than a five-membered cyclic structure. In addition, formation of the six-membered ring would involve a secondary radical intermediate in the propagation step, whereas the five-membered ring generates a primary radical, which is less stable. However, experimentally it has been reported that the monomers formed five-membered rings exclusively. [18, 19, 20, 21]

The purpose of this study is to investigate the correlation between the polymerizability trend of diallylamines and some of their descriptors derived from quantum chemical calculations. The method involves: (i) computational modeling of five diallylamines, namely *N*,*N*-diallylammine (DAA), *N*,*N*-diallylamine hydrochloride ($DAAH^+Cl^-$), diallyl dimethyl ammonium chloride (DADMAC), 4-(*N*,*N*-diallylamino) pyridine (DAAP), and 4-(*N*,*N*-diallylamino) pyridine hydrochloride ($DAAPH^+Cl^-$) (Fig. 1); (ii) correlation of experimental polymerizability to calculated monomeric descriptors such as charge distribution, energy barrier for cyclization, bond order, local softness values and HOMO–LUMO gaps; (iii) establishment of a mathematical relation between the polymerizability of the monomers, represented by the experimental value of their chemical shifts ($\Delta\delta$), and the descriptors derived from quantum chemical calculations. The ultimate goal indeed was to build up a sound means of predicting the polymerizability of *N*,*N*-substituted-diallylammonium halide monomers prior to their synthesis. It was further desirable to provide guiding information for experimentalists in their endeavor to synthesize the derivatives of *N*,*N*-dialkyl-*N*-2-(alkoxycarbonyl) allylammonium monomers.

Methodology

Computational

The most stable conformer for each of the selected diallylamine monomers shown in Scheme 1 was determined by carrying out a conformer search using the semiempirical PM3 [22, 23] method using the SPARTAN 5.1.1 [24] package. The counterions of the cationic monomers were excluded in the calculations. All possible stationary geometries for the structures located as minima along the potential energy surfaces were generated by free rotation around single bonds. The number of conformers for each compound is 3^n, where n is the number of C–C or C–N single bonds. Thus, one would have to deal with a very large number of conformers for a given compound. Analysis of the structures located as local minima along the potential energy surfaces revealed that appreciable changes in the geometry produced only slight changes in energy. Having decided not to consider the structure corresponding to the global minimum only, we focused on those structures that lie within a pre-selected energy threshold. Accordingly, we decided to consider the distribution of structures among energy levels within 3 kcal mol^{-1} from the global minimum. The probability for each conformer existing in the proposed energy range was calculated using the Boltzmann distribution. The population of states among energy levels was determined by:

$$N_i/N_j = e^{-(Ei-Ej)/kT} \quad (1)$$

where N_i and N_j refer to the population, E_i and E_j are the energies of states i and j, k is the Boltzmann constant and T is the temperature. The relative probability of each state was found by computing the ratio of N_i to N_T, where $N_T = \Sigma N_j = \Sigma\ e^{-Ej/kT}$. The next step was to calculate weighted averages for each descriptor by multiplying the relative probability of each energy state by the corresponding value of the descriptor (Table 2). This was followed by summing up over all states within 3 kcal mol^{-1} of the global minimum. The monomeric descriptors discussed in the following are Boltzmann averages derived from semiempirical calculations.

In the intramolecular propagating step of the polymerization reaction (Scheme 2), there is a long polymer chain at the first position. For simplicity, this initiated monomer has been modeled as if it had been initiated by an H radical and will be referred to as a "living monomer" (Fig. 1). To find the minimum energy conformer for this living monomer, a conformer search was performed along the potential energy surface for $DAAH^+$ using the SPARTAN 5.1.1 [24] package with the semiempirical PM3 method. Different substituents were inserted on nitrogen atom and then optimized, starting with the global minimum of the $DAAH^+$ geometry. These three-dimensional structures were used as representative living monomers (Fig. 1). To model the cyclization reaction and find the geometric, thermodynamic and kinetic

Table 2 The average electrostatic charges on atoms calculated with PM3

	DADMAC	$DAAH^+$	$DAAPH^+$	DAAP	DAA
C_1	–0.04	–0.03	–0.09	–0.16	–0.20
C_2	–0.26	–0.21	–0.22	–0.18	–0.18
C_1–C_2	*0.22*	*0.18*	*0.13*	*0.02*	*–0.02*
C_6	–0.17	–0.22	–0.21	–0.20	–0.22
C_7	–0.05	–0.03	–0.09	–0.15	–0.17
C_7–C_6	*0.12*	*0.19*	*0.12*	*0.05*	*0.05*
N	0.58	0.63	–0.10	–0.64	–0.76

Table 3 The heats of formation ΔH_f for the living monomer and the minimum energy transition state structures for the intramolecular cyclization reaction in kcal mol^{-1}

	DADMAC	DAAH$^+$	DAAPH$^+$	DAAP	DAA
$\Delta H_{f(reactant)}$	181.62	180.08	203.11	61.38	26.97
$\Delta H_{f(TS)}$	189.12	190.59	213.94	70.48	36.77

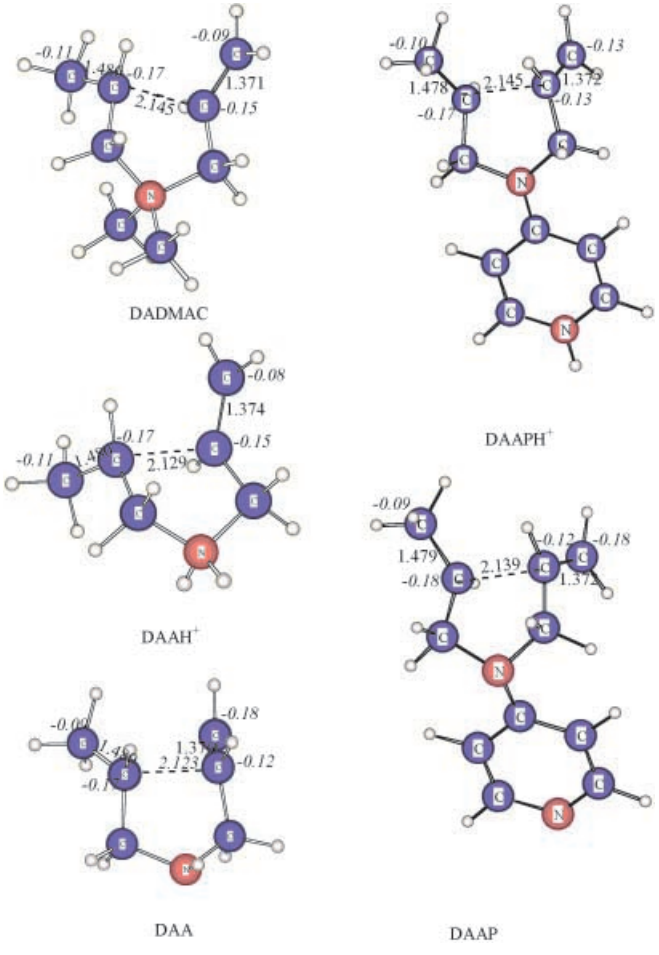

Fig. 2 The three-dimensional transition state structures of minimum activation energy for intramolecular cyclization reactions

parameters for the intramolecular cyclization reaction, these living monomers and the transition state structures for five- and six-membered cyclization reactions were located for all the monomers studied. All the plausible transition state structures, *cis* or *trans* orientations in the five-membered ring and chair or boat conformations in six-membered ring, were located. The nature of the transition state structures was confirmed by one imaginary frequency belonging to the forming bond. Nevertheless, the transition states with the minimum energy of activation (Table 3) were selected for each monomer since the reactions proceed along the lower barrier pathway. Figure 2 displays the three-dimensional structures of the transition states of minimum energy of activation with Mulliken charges on C_1, C_2, C_6, C_7, N and some critical distances.

Table 4 Bond orders for C_2–C_6, Fukui functions, S (global softness), $s^o(r)$ for C_6 and HOMO–LUMO gaps for the radical reactant and HOMO–LUMO gaps for propagating ring structure and the monomer

	DADMAC	DAAH$^+$	DAAPH$^+$	DAAP	DAA
Bond order for C_2–C_6	0.01103	0.01038	0.01028	0.00995	0.00989
$f(r)$[a] for C_6	0.075	0.075	0.05	0.07	0.06
S[b]	0.896	0.781	1.695	0.112	0.099
$s^o(r)$[c] for C_6	0.0672	0.0585	0.0847	0.0067	0.0069
ΔE_I[d]	1.117	1.281	0.590	8.918	10.138
ΔE_{II}[e]	–0.080	–0.039	0.015	8.997	10.346

[a] $f(r)$=Fukui function
[b] S=global softness
[c] $s^o(r)$=local softness
[d] ΔE_I=HOMO$_{reactant}$–LUMO$_{reactant}$
[e] ΔE_{II}=HOMO$_{ring}$–LUMO$_{monomer}$

The local and global softness calculations were performed on the monomers by using Mulliken atomic charges. The response of electron density at each point in space to the variation in the number of electrons is called the Fukui function ($f(r)$) by Parr and Yang. [25]

$$f(r) = \left(\frac{\partial \rho(r)}{\partial N}\right)_{v(r)} \quad (2)$$

$\rho(r)$ is the electron density, N is the number of electrons and $v(r)$ is the external potential acting on an electron. The Fukui function describes the sensitivity of a chemical potential of a system to a local perturbation.

The local softness, [26, 27] $s(r)$ is described as:

$$s(r)=f(r)S \quad (3)$$

where S represents global softness and is defined as;

$$S = \left(\frac{1}{IE - EA}\right) \quad (4)$$

where IE is the ionization energy and EA is the electron affinity of the molecule. $s(r)$ carries the same information as $f(r)$ and it has been widely used to understand the reactivity of an atom in a molecule. The local softness functions for a particular atom are:

$$s^+ = \left[\rho_{(No+1)} - \rho_{(No)}\right] \cdot S \quad \text{for nucleophilic attack} \quad (5)$$

$$s^- = \left[\rho_{(No)} - \rho_{(No-1)}\right] \cdot S \quad \text{for electrophilic attack} \quad (6)$$

$$s^o = 1/2\left[\rho_{(No+1)} - \rho_{(No-1)}\right] \cdot S \quad \text{for radical attack} \quad (7)$$

N_o is the number of electrons in the ground state of the system of interest and $\rho_{(No+1)}$, $\rho_{(No)}$ and $\rho_{(No-1)}$ represent the electronic population or the charge of the atom at the geometry of $\rho_{(No)}$. For the system of interest, Mulliken charges were used to calculate local softness values for C_6 where the radical attack will occur to form the five-membered ring. Although electrostatic charges were used to calculate the average charges in the monomers, it is common practice to use Mulliken charges to calculate local softness. The local softness values for C_6 are shown in Table 4.

In the intermolecular reaction, there is an attack from the ring structure to another monomer. The difference in energies of the HOMO of the incoming radical and LUMO of the allyl monomer have been analyzed in order to investigate an effective overlap between the two (Table 4). For the intramolecular reaction, the HOMO–LUMO energy differences of the representative living monomers have been also tabulated in Table 4.

Mathematical modeling

The correlation between the polymerizability of diallylamine monomers and their quantum chemical descriptors was established by constructing a non-linear regression model with one dependent and multiple independent variables. The dependent variable was defined as the chemical shift in β and γ carbons, taken from the experimental work of others. [16] The independent variables were made of a set of monomer-specific descriptors estimated by PM3 calculations and corresponding to the two symmetric structures around β and γ carbons, respectively. Hence, two models were defined for each monomer as:

$$\delta_\beta = A_\beta + B_\beta f(\mathrm{DES}_1)_\beta + C_\beta f(\mathrm{DES}_2)_\beta + D_\beta f(\mathrm{DES}_3)_\beta + \ldots. \quad (8)$$

$$\delta_\gamma = A_\gamma + B_\gamma f(\mathrm{DES}_1)_\gamma + C_\gamma f(\mathrm{DES}_2)_\gamma + D_\gamma f(\mathrm{DES}_3)_\gamma + \ldots. \quad (9)$$

where δ_β and δ_γ are the chemical shifts in β and γ carbons, respectively; $f(\mathrm{DES}_1)_{\gamma,\beta}$, $f(\mathrm{DES}_2)_{\gamma,\beta}$, $f(\mathrm{DES}_3)_{\gamma,\beta}$,... are linear or non-linear functions of the quantum chemical descriptors defined by DES_i; and $A_{\gamma,\beta}$, $B_{\gamma,\beta}$, $C_{\gamma,\beta}$, $D_{\gamma,\beta}$ are the parameters of the models, the subscripts referring to β and γ cases. The input data for the independent variables consisted of bond lengths, atomic charges, heats of formation and energy of activation. The statistical significance of each variable in terms of their contributions to the proposed correlation was tested within 95% confidence limits, and those variables with insignificant contributions were discarded from the model. Once the variables of the best representative model were selected, the model was tested for reliability by computing δ_β and δ_γ values of an arbitrarily selected diallylamine sample, using the estimated values of model parameters. All regression analyses were carried out by using the non-linear subroutine of a statistical program package. [28]

Discussion

Descriptors derived from calculations

It has been shown experimentally that the polymerizability trend depends on the nature of the substituents attached to nitrogen atom. [16] The structural parameters, bond orders, charges, heats of formation, local softness values and energy barriers to polymerization reaction were considered as plausible descriptors for the polymerizability of diallylamines. Throughout the discussion that follows, these descriptors will be discussed. The numbering system is the same as the one adopted in Scheme 1.

Charges

The average electrostatic charge on C_1 was found to decrease in the order: DAA>DAAP>$\mathrm{DAAPH^+}$> DADMAC>$\mathrm{DAAH^+}$ (Table 2). Since the experimental polymerizabilities of the monomers is in the reverse order (Table 1), [16] it follows that the smaller the electron density distribution on C_1, the better the polymerizability. The trend in experimental polymerizability is perfectly reproduced in our calculations except for the exchange in the orders of DADMAC and $\mathrm{DAAH^+}$, in which the charges on C_1 are very close (–0.04 and –0.03, respectively). The long-range delocalization of charges depends on the substituents such that the charge on C_1 is more positive for the most electron-withdrawing allylic substituent. The situation is similar for C_7, which is symmetric to C_1 (Scheme 1). The charge on C_7 reflects the polymerizability trend as in the case of C_1 and the orders of DADMAC and $\mathrm{DAAH^+}$ are interchanged again due to very close values of charge distributions (–0.05 and –0.03, respectively).

The electron density on C_2 was also found to be an indicator of polymerizability. The calculated charges on C_2 are given in the following order of increasing electron density: DADMAC>$\mathrm{DAAPH^+}$>$\mathrm{DAAH^+}$>DAAP=DAA. This order is in agreement with the experimental polymerizability trend, except for $\mathrm{DAAPH^+}$ and $\mathrm{DAAH^+}$ (whose orders are exchanged), in which electron distributions are almost equivalent (–0.21 and –0.22, respectively) (Table 2).

The C_6 preference for attack in the intramolecular cyclization is also confirmed by our calculations. The electrostatic charge distribution with PM3 calculations has shown that C_6 is richer in electrons than C_7. This can be interpreted in terms of the preference of the C_2 radical to attack the electron-rich center, C_6. The consequence of such a preference is an enhanced rate of cyclopolymerization (upon decreased rate of six-membered ring formation). Accordingly, the calculated charge difference between the vinyl carbons is an excellent replicator of the experimental polymerizability trend, shown in Table 2. As the electrostatic charge difference between C_1 and C_2 (C_1–C_2), and C_6 and C_7 (C_6–C_7) atom pairs increases, the polymerizabilities of the monomers of interest also increase. Hence, the difference of charges on double bond carbons was found to be higher for the monomers that polymerized well and lower for poorly polymerizing monomers.

Another indicator of polymerizability is the electrostatic charge on the nitrogen atom (Table 2). The calculated electrostatic charges on nitrogen atoms in order of decreasing electron densities are as DAA>DAAP> $\mathrm{DAAPH^+}$>DADMAC>$\mathrm{DAAH^+}$. This trend mimics the experimental tendency for polymerizability of the mono-

Table 5 Energetics and kinetics for the intramolecular cyclization reaction (T=298.150 K)

Energetic and kinetic data/substituent	DADMAC	$DAAH^+$	$DAAH^+$	DAAP	DAA
E_a[a] (kcal mol^{-1})	7.5	10.51	10.83	9.1	9.8
E_a+ZPE[b] (kcal mol^{-1})	7.88	10.45	10.50	11.67	9.61
$\Delta H^{\neq}$[c] (kcal mol^{-1})	6.78	9.61	9.85	10.39	8.79
$\Delta H^{\neq}$+ZPE[d] (kcal mol^{-1})	7.16	9.55	9.52	12.96	8.60
$\Delta S^{\neq}$[e] (cal mol K^{-1})	–13.02	–9.98	–7.49	–12.38	–9.38
$\exp(-E_a/RT)$	3.18×10^{-6}	1.97×10^{-8}	1.15×10^{-8}	2.13×10^{-7}	6.54×10^{-8}
$\exp(-E_a+\mathrm{ZPE}/RT)$	1.67×10^{-6}	2.18×10^{-8}	2.02×10^{-8}	2.79×10^{-9}	9.02×10^{-8}
$\exp(-\Delta H^{\neq}/RT)$	1.07×10^{-5}	9.02×10^{-8}	6.01×10^{-8}	2.40×10^{-8}	3.60×10^{-7}
$\exp(-\Delta H^{\neq}+\mathrm{ZPE}/RT)$	5.64×10^{-6}	9.98×10^{-8}	1.06×10^{-7}	3.14×10^{-10}	4.96×10^{-7}
$\exp(-E_a/RT)\exp(\Delta S^{\neq}/RT)$	4.53×10^{-9}	1.30×10^{-10}	2.65×10^{-10}	4.20×10^{-10}	5.83×10^{-10}
$\exp(-E_a+\mathrm{ZPE}/RT)\exp(\Delta S^{\neq}/RT)$	2.39×10^{-9}	1.44×10^{-10}	4.67×10^{-10}	5.48×10^{-12}	8.03×10^{-10}
$\exp(-\Delta H^{\neq}/RT)\exp(\Delta S^{\neq}/RT)$	1.53×10^{-8}	5.94×10^{-10}	1.39×10^{-9}	4.73×10^{-11}	3.21×10^{-9}
$\exp(-\Delta H^{\neq}+\mathrm{ZPE}/RT)\times\exp(\Delta S^{\neq}/RT)$	8.04×10^{-9}	6.57×10^{-10}	2.44×10^{-9}	6.17×10^{-13}	4.42×10^{-9}

[a] E_a=activation energy
[b] E_a+ZPE=activation energy with zero-point energy
[c] $\Delta H^{\neq}$=enthalpy of activation
[d] $\Delta H^{\neq}$+ZPE=enthalpy of activation with zero-point energy
[e] $\Delta S^{\neq}$=entropy of activation

mers. Vaidya et al. have also correlated the electron-withdrawing ability of allylic substituents with their polymerizabilities. [16] The electrostatic charge on nitrogen is indicative of the electron-withdrawing ability of the monomer. The order of decreasing nitrogen charges in the studied monomers reflects the decreasing electron-withdrawing capacity, implying also a decreasing trend in polymerizability. As in the case of C_1, C_7 and C_2, the orders were exchanged for the case of $DAAH^+$ and DADMAC.

Energetics and rate

The minimum energy structures for the transition states of the cyclization reaction are displayed in Fig. 2. In all the monomers studied, the C–C distance for the forming bond in the transition state structures is ~2.1 Å. The plausible transition state structures for five- and six-membered rings leading to cyclization reactions have higher heats of formation for six-membered ring formation. Except for DAA, all the monomers have the lowest heat of formation of transition state structure for five-membered ring formation as shown by experiments [18, 19, 20, 21] (Table 5). Additionally, it was reported experimentally that the rings had a *cis*:*trans* ratio of 6:1 [29, 30, 31] and 3–4:1 [32] for DADMAC in different studies. With the semiempirical PM3 calculations, the dominating ring streochemistry was *trans*, in contrast to experimental findings.

The activation energies, calculated by using the energetics of transition states, were considered as indicators of barriers to cyclization reactions. The activation energies for DADMAC, $DAAH^+$ and $DAAPH^+$ reproduced the polymerizability trend (Table 5). The trend was further improved when the zero-point energies were taken into account, except for DAA, which did not fit into the expected trend. The enthalpy of activation showed the same trend as the energy of activation. The entropies of activation, $\Delta S^{\neq}$, were also calculated to see their effect on the pre-exponential factor, A, in the rate equation. The rate of a reaction is described as:

$$\mathrm{Rate}=A\mathrm{e}^{-E_{a/RT}} \tag{10}$$

The pre-exponential factor, A, is proportional to the entropy of activation exponentially, such as:

$$A=\frac{kT}{h}\frac{RT}{p}\mathrm{e}^{\frac{\Delta S^{\neq}}{R}}\mathrm{e}^{2} \tag{11}$$

where k is the Boltzmann constant and h is Planck's constant. The product of the pre-exponential factor with the exponential factor did not reproduce the expected trend qualitatively. It may be that the entropy does not play a significant role in predicting the rate of polymerization or the rigid rotor and harmonic oscillator approximations used in calculating the thermodynamic parameters are not adequate approximations for the molecules selected.

Bond order

The bond order of the forming bond between C_2 and C_6 atoms, in the intramolecular cyclization reaction of the propagating living monomer, was in the order of 0.01103, 0.01038, 0.01028, 0.0995 and 0.0989 for DADMAC, $DAAH^+$, $DAAPH^+$, DAAP and DAA (Table 4), respectively. These values indicate that the higher the bond order, the more eager the monomer is for bond formation and the more polymerizable it is.

Local softness

One of the descriptors of polymerizability was found out to be the local softness (s^o), tabulated in Table 4. The local softness values of C_6, which is the site of attack for the five-membered ring formation in the cyclization reaction, showed that there was a tenfold decrease from monomers of high polymerizability to

low polymerizability. This indicated the sensitivity of C_6 to a radical attack and hence reproduced the polymerizability trend.

HOMO–LUMO gaps

The HOMO–LUMO difference in a chemical system can be considered a measure of its resistance to changes in electronic configuration. Large HOMO–LUMO gaps are known to provide great stability and low reactivity to a chemical species. In the intramolecular propagating step of polymerization reaction, there is a transfer of the unpaired electron from the incoming radical to the olefinic bond. This transfer is accomplished by mixing of the α-odd electron with the LUMO of olefinic bond. The HOMO–LUMO energy differences for the propagating living monomer, ΔE_I, are much larger for monomers polymerizing poorly whereas this difference is quite small for good polymerizing monomers (Table 4).

In the intermolecular step during polymerization, the HOMO from the propagating radical ring structure, which is the electron donor, will interact with another monomer, which is the acceptor. This HOMO–LUMO interaction will take place more efficiently when the energy gap between the two molecular orbitals, $\Delta E_{II,}$ is small. The gap between the HOMO of the five-membered ring and the LUMO of the unattacked diallyl monomer reflects the polymerization trend perfectly. The gap is very small for monomers of high polymerizability, indicative of easier mixing of these orbitals. The gap is significantly larger for monomers of low polymerizability.

Table 6 Final input data for estimating model parameters

Monomer	Dependent variable		Independent variables		
	δ_γ	δ_β	DES_1 (C1C7)	DES_2 (C2C6)	DES_3 (*N*)
DADMAC	125.4	128.4	–0.05	–0.22	+0.58
$DAAH^+$	125.0	128.1	–0.03	–0.22	+0.63
$DAAPH^+$	118.3	130.7	–0.09	–0.22	–0.10
DAAP	115.3	131.7	–0.16	–0.19	–0.64
DAA	117.6	136.7	–0.19	–0.20	–0.76

Table 7 Model outputs

Model	*f*(DES_n)						
	DES_1	DES_2	DES_3	*A*	*B*	*C*	*D*
I (γ-shift)	C1C7	$C2C6^2$	*N*	103.08	–134.61	111.39	19.68
II (β-shift)	$C1C7^2$	C2C6	*N*	91.16	315.60	–171.76	–0.50

Correlation of monomeric descriptors with polymerizability

The input data for estimating the parameters of the proposed models initially consisted of all the calculated descriptors of the five diallylamines and the experimentally determined chemical shifts of the β and γ carbons. In the first step, a stepwise regression analysis was performed to exclude those descriptors (if any) with statistically insignificant contributions to the proposed models, represented by Equations 2 and 3. In accordance, it was found that the only significantly contributing descriptors were the electrostatic charges on C_1, C_2, C_6, C_7 and N. Furthermore, the model was found to improve statistically when the carbon-related charge variables were represented by two arithmetic means: as that of C_1 and C_7 (named C1C7) and C_2 and C_6 (named C2C6). The reduced set of input variables after elimination of non-contributing independent variables is presented in Table 6. Note that variable *N* represents the charge on nitrogen.

The output data for the proposed models (to predict δ_β and δ_γ) are presented in Table 7 in terms of charge descriptor functions and the estimated parameters.

Results of variance analysis, standard errors of estimate and regression coefficients for the predicted correlations are summarized in Table 8.

In summary, the predicted correlation between the polymerizability of a diallyl monomer (in terms of the shift in γ- and/or the β-carbon) and the quantum chemical descriptors is defined by:

$$\delta_\gamma = 103.08 - 134.61(C1C7) + 111.39(C2C6)^2 + 19.68(N) \quad (r^2 = 0.989) \tag{12}$$

$$\delta_\beta = 91.16 + 315.60(C1C7)^2 - 171.76(C2C6) - 0.50(N) \quad (r^2 = 1.00) \tag{13}$$

where *N* represents the electrostatic charge on the nitrogen atom of the monomer.

In observing the values in Table 8, it appears that the second model (developed for the β-carbon-shift) is a better predictor of polymerizability in terms of statistical significance. However, a test of the two models on a diallylamine monomer outside our sample population, namely *N*,*N*,*N*-triethyl-*N*-allylammonium bromide, showed that the predicted shifts by both models are very close to

Table 8 Analysis of variance and correlation coefficients

Model	Sum of squares		Mean square		Corrected R^2	Standard error			
	Regression	Residual	Regression	Residual		*A*	*B*	*C*	*D*
I (δ_γ)	72468.7	0.227	18117.2	0.227	0.989	4.99	21.84	95.03	2.20
II (δ_β)	86010.2	0.003	21502.6	0.003	1.00	0.97	6.33	4.56	0.14

Table 9 The result of test and the input data for test monomer, *N*,*N*,*N*-triethyl-*N*-allylammonium bromide

Monomer	Charges			Chemical shifts			
				Predicted		Observed	
	C1C7	C2C6	*N*	γ	β	γ	β
	–0.03	–0.23	0.66	126.0	130.62	125.1	128.9

the actual values. The results of this test and the input data for the monomer are presented in Table 9.

Conclusion

The aim of this project was to correlate the experimental cyclopolymerizability trend of a series of diallylamine monomers by the descriptors derived from quantum mechanical calculations. Hence, it is possible to make predictions for monomers that have not yet been synthesized. The ^{13}C NMR chemical shifts of the diallylamine monomers studied, which have been correlated to the polymerizabilities, [16] could be correlated successfully to the descriptors derived from calculations. The "weighted average" charges of vinyl carbons and nitrogen could successfully reproduce the polymerizability trend. The activation energies and the enthalpy differences between the transition state structures and the living monomers for the intramolecular cyclization reproduced the polymerizability trend successfully in general. DFT calculations are in progress in order to test how activation energies calculated with a more sophisticated method will reproduce the experimentally observed polymerizability trend. The C_2–C_6 bond order, local softness values of C_6 and HOMO–LUMO gaps were also found to reflect the polymerizabilities of the monomers. The mathematical model predicts ^{13}C NMR chemical shifts based on electrostatic charges derived from quantum mechanical calculations (PM3). Although the model has been developed with only five samples, the validation check has shown that the model is acceptable. Data on similar monomers will be desired in order to extend the usage of the proposed model.

Acknowledgements The authors gratefully acknowledge the support of Boğaziçi University Araştirma Fonu Project 00B501D. N.Ş. Tüzün is indebted to TUBITAK for the NATO-A1 grant which has enabled her stay at UCLA.

References

1. Butler GB, Bunch RL (1949) J Am Chem Soc 71:3120
2. Wandrey C, Hernandez-Barajas J, Hunkele D (1999) Adv Polym Sci 145:123
3. Antonetti JM, Snow GF (1979) US Patent 4,141,691
4. Sykes RC, Connelly RJ, Roe WJ (1985) US Patent 4,555,329
5. Kerr EM, Ramesh M (1997) US Patent 5,622,647
6. Biermann CJ (1996) Handbook of pulping and papermaking. Academic Press, San Diego, Calif.
7. Jansma RH, Begala AJ, Furman GS (1996) US Patent 5,490,904
8. Wandrey C, Jaeger W, Starke W, Wotzka J (1984) Wasserwirtsch Wassertech 34:18
9. Bhattacharyya BR, Srivatsa SR, Dwyer ML (1987) US Patent 4,715,962
10. Chung DK, Ramesh M (1997) US Patent 5,597,490
11. Chung DK, Ramesh M (1997) US Patent 5,624,569
12. Sivakumar A, Ramesh M (1996) U S Pat 5,560,832
13. Dautzenberg H, Jaeger W, Kotz J, Philipp B, Seidel C (1994) Polyelectrolytes. Formation, characterization, application. Carl Hanser, Muenchen
14. Mandel M (1988) Encyclopedia of Polymer Science, vol 11. Wiley, New York, p 739
15. Zubov VP, Vjaya Kumar M, Masterova MN, Kabanov VA (1979) J Macromol Sci, Chem 13:111
16. Vaidya RA, Mathias LJ (1986) J Polym Sci, Polym Symp 74:243
17. Avcı D, Küsefoğlu SH, Thompson RD, Mathias LJ (1994) J Polym Sci, Polym Chem Ed 32:2937
18. Lancaster JE, Bacchei L, Panzer HP (1976) J Polym Sci, Polym Lett Ed 14:549
19. Ottenbride RM, Shillady DD (1980) In: Goethals E (ed) Polymeric amines and ammonium salts. Pergamon, Oxford, p 143
20. Wandrey C, Jarger W, Reinish G, Hahn M, Engelhard G, Jancke H, Ballschuh D (1981) Acta Polym 32:179
21. Masterman TC, Dando NR, Weaver DG, Seyferth D (1994) J Polym Sci, Part B: Polym Phys 32:2263
22. Stewart JJP (1989) J Comput Chem 10:209
23. Stewart JJP (1989) J Comput Chem 10:221
24. SPARTAN Version 5.1.1. Wavefunction, Irvine, CA 92715
25. Parr RG, Yang W (1984) J Am Chem Soc 106:4049
26. Yang W, Parr RG (1985) Proc Natl Acad Sci USA 82:6723
27. Berkowitz M, Parr RG (1988) J Chem Phys 88:2554
28. Willkinson L (1987) In: Evanston IL (ed) The system for statistics. SYSTAT, Chicago, Il.
29. Lancester JE, Bacchei L, Panzer HP (1976) J Polym Sci, Polym Lett Ed 14:549
30. Ottenbride RM, Shillady DD (1980) In: Goethals E (ed) Polymeric amines and ammonium salts. Pergamon, Oxford, p 125
31. Wandrey C, Jarger W, Reinish G, Hahn M, Engelhard G, Jancke H, Ballschuh D (1981) Acta Polym 32:179
32. Masterman TC, Dando NR, Weaver DG, Seyferth D (1994) J Polym Sci, Part B: Polym Phys 32:2263